

01 Aug 2011

## Sol-Gel Derived Silver-Incorporated Titania Thin Films on Glass: Bactericidal and Photocatalytic Activity

Betul Akkopru Akgun

Anthony W. Wren


Caner Durucan

Mark R. Towler

*Missouri University of Science and Technology*, mtowler@mst.edu

*et. al.* For a complete list of authors, see [https://scholarsmine.mst.edu/che\\_bioeng\\_facwork/1165](https://scholarsmine.mst.edu/che_bioeng_facwork/1165)

Follow this and additional works at: [https://scholarsmine.mst.edu/che\\_bioeng\\_facwork](https://scholarsmine.mst.edu/che_bioeng_facwork)

 Part of the [Biochemical and Biomolecular Engineering Commons](#), and the [Biomedical Devices and Instrumentation Commons](#)

---

### Recommended Citation

B. A. Akgun et al., "Sol-Gel Derived Silver-Incorporated Titania Thin Films on Glass: Bactericidal and Photocatalytic Activity," *Journal of Sol-Gel Science and Technology*, vol. 59, no. 2, pp. 228 - 238, Springer, Aug 2011.

The definitive version is available at <https://doi.org/10.1007/s10971-011-2488-6>

This Article - Journal is brought to you for free and open access by Scholars' Mine. It has been accepted for inclusion in Chemical and Biochemical Engineering Faculty Research & Creative Works by an authorized administrator of Scholars' Mine. This work is protected by U. S. Copyright Law. Unauthorized use including reproduction for redistribution requires the permission of the copyright holder. For more information, please contact [scholarsmine@mst.edu](mailto:scholarsmine@mst.edu).

# Sol–gel derived silver-incorporated titania thin films on glass: bactericidal and photocatalytic activity

Betul Akkopru Akgun · Anthony W. Wren ·  
Caner Durucan · Mark R. Towler ·  
Nathan P. Mellott

Received: 1 February 2011 / Accepted: 7 May 2011 / Published online: 19 May 2011  
© Springer Science+Business Media, LLC 2011

**Abstract** Titanium dioxide (TiO<sub>2</sub>) and silver-containing TiO<sub>2</sub> (Ag-TiO<sub>2</sub>) thin films were prepared on silica pre-coated float glass substrates by a sol–gel spin coating method. The bactericidal activity of the films was determined against *Staphylococcus epidermidis* under natural and ultraviolet (UV) illumination by four complementary methods; (1) the disk diffusion assay, (2) UV-induced bactericidal test, (3) qualitative Ag ion release in bacteria inoculated agar media and (4) surface topographical examination by laserscan profilometry. Photocatalytic activity of the films was measured through the degradation of stearic acid under UV, solar and visible light conditions. The chemical state and distribution of Ag nanoparticles, as well as the structure of the TiO<sub>2</sub> matrix, and hence the bactericidal and photocatalytic activity, is controlled by post-coating calcination treatment (100–650 °C). Additionally, under any given illumination condition the Ag-incorporated films were found to have superior bactericidal and photocatalytic activity performance compared to TiO<sub>2</sub> thin films. It is shown that with optimized thin film processing parameters, both TiO<sub>2</sub> and Ag-TiO<sub>2</sub> thin films

calcined at 450 °C were bactericidal and photocatalytically active.

**Keywords** Titania · Thin film · Silver nanoparticle · Antibacterial · Antimicrobial · Photocatalytic

## 1 Introduction

Titanium dioxide (TiO<sub>2</sub>) has been widely used as a photocatalyst due to its high photocatalytic efficiency, corrosion resistance and relatively low cost. Upon UV light irradiation, valence band electrons in TiO<sub>2</sub> are excited into the conduction band creating an electron–hole (e<sup>-</sup>/h<sup>+</sup>) pair. The electron hole pairs migrate to the surface to produce powerful oxidizing species or superoxide radicals [1, 2]. These oxidizing species effectively breakdown a wide variety of organic species including contaminant molecules, fungi, and bacteria. The wide band gap of TiO<sub>2</sub> (~3.2 eV) limits the use of the catalyst to ultraviolet light irradiation conditions. Numerous studies have been carried out to increase the photo-efficiency of TiO<sub>2</sub> and to develop visible light activity of TiO<sub>2</sub> including; (1) formation of surface defects, (2) anion doping, and (3) metal doping. Of particular interest here is the doping of TiO<sub>2</sub> with Ag. The improvement in functional performance with incorporation of Ag in the metallic (Ag<sup>0</sup>) and/or oxide form (Ag<sub>x</sub>O<sub>y</sub>) into the TiO<sub>2</sub> matrix can be explained in terms of a charge separation model and higher production rate of photogenerated (e<sup>-</sup>/h<sup>+</sup>) pairs [3–7]. As the fermi level of TiO<sub>2</sub> is higher than that of Ag, the Ag deposits behave as accumulation sites for photogenerated electrons derived from TiO<sub>2</sub>, leading to better separation of electrons and holes. This results in a higher number of charge carriers and hence an increase in reactive species. The yield of (e<sup>-</sup>/h<sup>+</sup>)

**Electronic supplementary material** The online version of this article (doi:10.1007/s10971-011-2488-6) contains supplementary material, which is available to authorized users.

B. A. Akgun · C. Durucan  
Department of Metallurgical and Materials Engineering, Faculty of Engineering, Middle East Technical University, 06531 Ankara, Turkey

B. A. Akgun · A. W. Wren · M. R. Towler · N. P. Mellott (✉)  
Department of Materials Science and Engineering, Inamori School of Engineering-NYSCC, Alfred University, Alfred, NY 14802, USA  
e-mail: mellott@alfred.edu

pairs can also be increased through incorporation of Ag into TiO<sub>2</sub> by the generation of local electric fields due to surface plasmon resonance of Ag particles [8, 9].

The preparation method of Ag-TiO<sub>2</sub> is critical for achieving a uniform distribution of Ag and controlling the chemical interaction between Ag and TiO<sub>2</sub>, as these factors will determine the final performance properties (bactericidal and photocatalytic activities). The sol–gel method enables control of the size, distribution, and chemical state of Ag, as well as the crystal phase and morphology of the host TiO<sub>2</sub> matrix; all of which affect the final performance properties. Ag can be introduced into the TiO<sub>2</sub> matrix, by dissolving a silver salt in the initial sol followed by subsequent reduction of Ag<sup>+</sup> ions to metallic particles via either photochemical [10, 11] or thermal [6, 12, 13] treatment. It has been shown that Ag does affect the overall structure and chemistry of TiO<sub>2</sub>. It is unclear how process parameters such as calcination temperature and presence of Ag influence the bactericidal and photocatalytic activity. Thus, establishment of a correlation between structural, chemical, and performance properties (bactericidal and photocatalytic activities) of Ag-TiO<sub>2</sub> thin films is crucial.

The effect of Ag incorporation and calcination temperature on microstructure of the TiO<sub>2</sub> matrix, the chemical state of Ag, and its distribution in the host matrix was investigated. The bactericidal activity of the coatings was determined against *Staphylococcus epidermidis* (*S. epidermidis*) under both UV and natural light. Furthermore, photocatalytic activity of films was examined under UV light, solar light and visible light conditions, through monitoring the photodegradation of stearic acid via fourier transformed infrared (FTIR) spectroscopy. A specific objective of this study was to determine the changes in bactericidal and photocatalytic activity as a result of structural and chemical changes of the film surface with incorporation of Ag and modification of calcination temperature. The effect of Ag incorporation and calcination temperature on the efficiency of *S. epidermidis* termination and stearic acid removal on TiO<sub>2</sub> films are presented.

## 2 Materials and methods

### 2.1 Preparation and characterization of TiO<sub>2</sub> and Ag-TiO<sub>2</sub> thin films

#### 2.1.1 Sol preparation

TiO<sub>2</sub> and Ag-TiO<sub>2</sub> sols were prepared starting from titanium-n-butoxide (Ti[O(CH<sub>2</sub>)<sub>3</sub>CH<sub>3</sub>]<sub>4</sub>, TNBT, Aldrich), silver nitrate (AgNO<sub>3</sub>, Aldrich), ethanol (C<sub>2</sub>H<sub>5</sub>OH, or EtOH, Merck), deionized (DI) water, and nitric acid (HNO<sub>3</sub>, Merck). For the preparation of the TiO<sub>2</sub> sol, 6 mL of

TNBT was slowly added to 7 mL EtOH (previously adjusted to pH1 via 1 M aqueous HNO<sub>3</sub>). Then, 6 mL DI-water was added dropwise into the TNBT/EtOH/HNO<sub>3</sub> solution and stirred for 30 min to obtain the final TiO<sub>2</sub> coating sol. This resulted in a precipitate free, visually homogeneous solution. For the Ag-TiO<sub>2</sub> sol preparation, an initial TiO<sub>2</sub> sol (TNBT/EtOH/water) was prepared by the method described above, however, using only 4 mL of DI-water. Then, 0.2 g of AgNO<sub>3</sub> was dissolved in 2 mL of DI-water in another beaker and stirred for 20 min. This Ag-containing solution was then added into the TiO<sub>2</sub> solution under stirring and further mixed for 100 min. The resultant sol was clear, precipitate free and stable up to 20 days. Typically, coating sols were aged for 24 h prior to coating.

#### 2.1.2 Coating process

Thin films were deposited on silica barrier-layer coated float glass substrates, pre-cleaned in acetone at 70 °C and blown with nitrogen. The single barrier-layer silica coating was prepared by a sol–gel spin coating method with details discussed elsewhere [14]. TiO<sub>2</sub> and/or Ag-TiO<sub>2</sub> coating sols were deposited onto cleaned substrates (typically 25 × 25 mm) by spin coating. Approximately 0.6 mL of the coating sol was placed on the substrate surface and spun at 2300 rpm for 30 s using a spin coater (Chemat Technology). The resultant samples were dried in an oven, under atmospheric conditions, at 100 °C for 1 h. This coating process was repeated three times. Transparent and colorless thin films were obtained. Finally, after the third coating, thin films were calcined in air at 250, 450 and 650 °C for 6 h and cooled to room temperature.

#### 2.1.3 Thin film characterization

Thin films used in this study were thoroughly characterized, as discussed in detail elsewhere [15]. However, it is worth summarizing the relevant analytical methods here. Phase identification was carried out by glancing incidence x-ray diffraction (GIXRD) studies performed using a Siemens D-500. The X-ray source was CuK $\alpha$  radiation at 40 kV. Step size and hold time was 0.04° and 40 s, respectively. The surface chemical analyses of the thin films were carried out using SPECS ESCA x-ray photoelectron spectrometer (XPS) with Mg/Al dual anode system employing Al K $\alpha$  at 20 mA anode current of an electron accelerating voltage of 15 kV with a pass energy of 55 eV and a step size of 0.1 eV. Both survey scans and individual high-resolution scans for Ag(3d) and Ti(2p) spectral regions were recorded. Binding energies have been corrected according to the C(1s) signal position (284.6 eV).

## 2.2 Bactericidal activity tests

The overall bactericidal activity was assessed using four complementary tests; (1) disk diffusion assay method, (2) UV-induced bactericidal test, (3) qualitative Ag ion release test and (4) laserscan profilometry. All bactericidal tests were performed under ambient, visible light conditions except for the second method, in which the bactericidal activity of Ag-TiO<sub>2</sub> thin films were determined under weak UV exposure.

### 2.2.1 Disk diffusion assay

The bactericidal activity of the TiO<sub>2</sub> and Ag-TiO<sub>2</sub> thin films were assessed by the disk diffusion assay against *S. epidermidis* under ambient light. All polystyrene dishes, glass bottles and materials were sterilized in an autoclave prior to experiment. Preparation of the agar disk diffusion plates involved seeding BHI agar plates with a sterile swab dipped in a 1/50 dilution of the appropriate 16 h culture of bacteria. Three samples of each material were placed on the inoculated plates and the plates were cultured for 36 h at 37 °C aerobically. The agar diffusion test was performed under standard laboratory sterile conditions where bacteria were handled under a fumigation hood using sterile cotton swabs.

Agar plates were used as a physical seeding media for bacteria culture and were required in order to achieve an effective and long-term contact between the thin film coated glass samples (typically 1.25 × 1.25 cm in size) and the bacteria.

Representative thin film coated glass samples were placed face up in polystyrene petri dishes and 25 mL of viscous agar (~100 °C) was poured onto the surface, completely covering the sample. Agar plates containing submerged samples were allowed to cool to 25 °C in air and were then inoculated with the 1/50 bacterial stock by spread plating with sterile swabs. A bare glass substrate was used as the control sample in all bactericidal tests. After 24 h of incubation at 37 °C, the inhibition zones (in mm) were determined by measuring the diameter of each disk at three cross-sectional cuts with average zone sizes determined using:

$$\text{Inhibition zone (in mm)} = [A - B]/2$$

where *A* is the total diameter of inhibition zone (mm), *B* is the cross-sectional linear dimension (mm) of the respective thin film coated glass sample.

### 2.2.2 UV-induced bactericidal test

The same bacteria culture and agar plate preparation procedures described above were used in the UV-induced

bactericidal tests. In a typical test, 250 μL of diluted bacterial culture was transferred onto the sample surface by micropipette and spread with a sterile swab. Then, bacteria culture coated samples were put into a closed polystyrene petri dish and irradiated from top (at a distance of 3 cm) for 3, 6 and 12 h with UV light ( $\lambda \sim 365$  nm) with an intensity of 0.02 mW/cm<sup>2</sup>. Then, the remaining solution on each sample was recollected with a sterile swab and inoculated onto preformed bacteria-free agar plates (*n* = 3) in separate polystyrene petri dishes. The formation of (or lack there-of) bacterial colonies on each plate was then examined visually after 24 h of incubation at 37 °C. It is worth noting that bare glass samples were also tested in the same manner to understand the inherent effect of UV light exposure on the resilience of the bacteria. The termination efficiency of bacterial colonies on thin film coated samples were compared to bacteria colony reduction on bare glass (control) samples.

### 2.2.3 Qualitative Ag ion release test

Bactericidal properties of the Ag-TiO<sub>2</sub> thin films were also evaluated based on their Ag<sup>+</sup> release into the bacteria-inoculated agar during the standard disk diffusion assay. This was performed by cross-sectional surface chemical compositional analysis (via XPS) of the representative agar strips exposed to Ag-TiO<sub>2</sub> thin films for 24 h at 37 °C. Two sets of strips of *S. epidermidis* seeded agar plates, employed in disk diffusion assays, hosting TiO<sub>2</sub> and Ag-TiO<sub>2</sub> films were examined. The first set of the agar strips were those in contact (for 24 h at 37 °C under ambient light) with TiO<sub>2</sub> films calcined at 250, 450 and 650 °C. The *second set* test strips were obtained from agar plates that had been in contact with Ag-TiO<sub>2</sub> films calcined at 250, 450 and 650 °C under identical conditions. Representative agar samples used in XPS analyses were 1 mm thick strips (10 mm × 20 mm) cut from the region in close proximity to the sample-agar contact, extending from the coated glass sample, through the inhibition zone (if any) up to the bacterial colonies. The strips were placed on a glass slide and dried at 37 °C in an oven (air atmosphere) for 24 h prior to XPS analysis. The XPS examinations of the agar strips were performed according to the same analysis/instrumental details as described above.

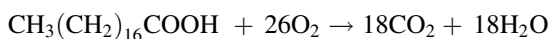
### 2.2.4 Laserscan profilometry

Laserscan profilometry analysis was carried out to determine the presence or absence of bacteria at the sample-agar border used in the standard disk diffusion assay (against *S. epidermidis* for 24 h at 37 °C under ambient light). In particular, the sample surface and the agar environments for the control sample (single silica layer coated float

glass), TiO<sub>2</sub> and Ag-TiO<sub>2</sub> thin films calcined at 450 °C were examined. Laser profilometry was performed on a Solarius Laserscan Profilometer (Solarius, CA USA), with a vertical sensor resolution of 0.1 μm and spot size of 2 μm. Analysis of data was operated using Solar Map version 5.0.4.5261 software.

### 2.3 Photocatalytic performance measurements

The photocatalytic activity of the thin films under UV light ( $\lambda \sim 365$  nm) simulated solar light (AM1.5) and visible light ( $\lambda = 400\text{--}700$  nm) were determined by measuring the degradation of a stearic acid layer deposited on the film surface. Stearic acid was selected as the model organic pollutant given it is non-volatile at room temperature and durable to UV light irradiation [16]. Photodegradation of stearic acid on TiO<sub>2</sub> surface under a photoirradiation with an energy higher than the band gap energy of TiO<sub>2</sub> ( $\sim 3.2$  eV) can be described with the following chemical equation [16]:



The degradation of stearic acid was monitored by FTIR spectroscopy using intensity of the absorption bands of stearic acid positioned at 2917 and 2848 cm<sup>-1</sup>; assigned to the asymmetric and symmetric C–H stretching modes, respectively. Therefore, the intensity and integratable area of these two bands are a function of the amount of stearic acid. A Thermo Nexus 6700 infrared spectrometer was used with spectra collected within the 2700–3100 cm<sup>-1</sup> range with a 0.5 cm<sup>-1</sup> step size. The integrated area of the absorbance bands was determined as a function of irradiation time.

In a typical photocatalytic performance test, thin film-coated test samples (25 × 25 mm in size) were pre-treated with UV light for 2 min. Then, 1 mL of stearic acid-methanol solution (obtained by dissolving 1 g stearic acid in 100 mL methanol) was deposited on the film surface and spun at 2300 rpm for 20 s. Following spin coating, stearic acid coated samples were irradiated using 50 W lamp at different wavelengths (UV, solar and visible light). In all cases, the distance between light source and sample surface was 6 cm. For ease of comparison of photocatalytic performance of the different samples, measured integrated absorbance values were normalized to the initial (pre-irradiation) absorbance. The percentage of stearic acid remaining (R%) as a function of illumination time was calculated according to:

$$R\% = [(A_0 - A_t)/A_0] \times 100$$

where  $A_0$  and  $A_t$  are the absorbance at time of 0 and  $t$ , respectively.

## 3 Results

### 3.1 Structural and chemical characterization of thin films

#### 3.1.1 Phase analysis by GIXRD

Figure 1 shows the GIXRD diffractograms of the TiO<sub>2</sub> (Fig. 1a) and Ag-TiO<sub>2</sub> (Fig. 1b) films after calcination at 250, 450, and 650 °C. The TiO<sub>2</sub> film calcined at 250 °C has a broad, featureless pattern suggesting an amorphous structure. The increase in calcination temperature to 450 °C leads to appearance of three well defined crystalline peaks centered at 25.3°, 38.6°, 48.1° 2θ as well as a peak doublet at around ~54–55° 2θ; all attributed to anatase (JCPDS 21-1272). Further increase in calcination

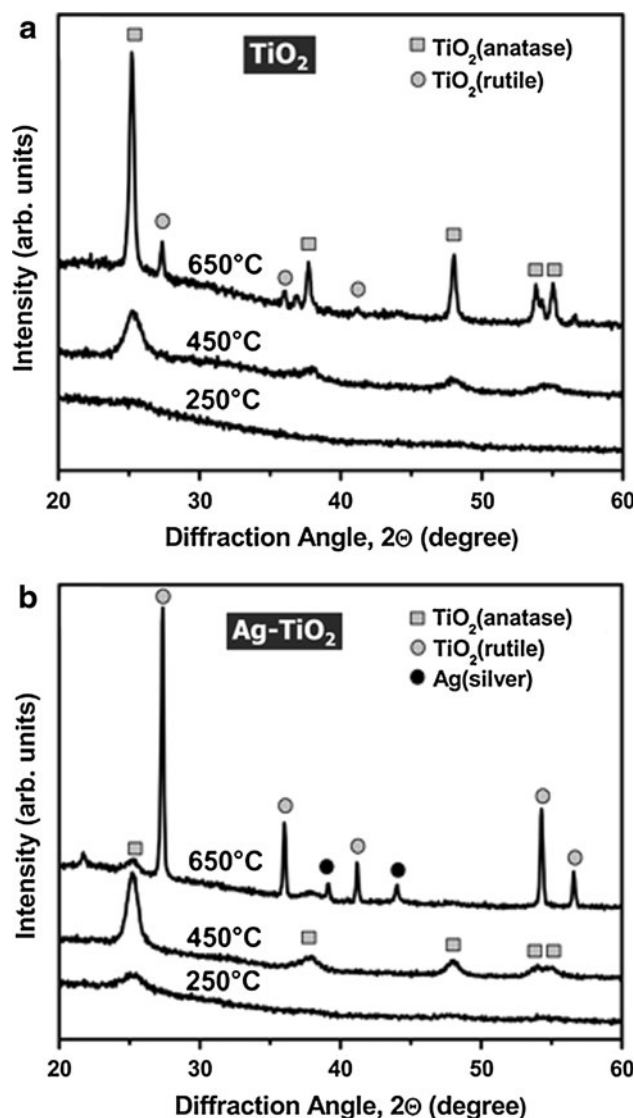


**Fig. 1** GIXRD diffractograms for **a** TiO<sub>2</sub>, **b** Ag-TiO<sub>2</sub> thin films calcined 250, 450 and 650 °C



temperature to 650 °C, results in a sharp increase in the intensity of all anatase peaks, accompanied by appearance of three additional peaks at 27.4°, 41.2° and 44.1° 2 $\theta$  to rutile (JCPDS 21-1276).

A broad, yet clear peak is observed at 25.3° 2 $\theta$  for the Ag-TiO<sub>2</sub> thin film after calcination at 250 °C; corresponding to early stages of anatase crystallization. The increase in calcination temperature to 450 °C leads to a well defined peak centered at 25.3° and additional peaks at 38.6°, 48.1° 2 $\theta$ , as well as a peak doublet at around ~54–55° 2 $\theta$ ; all attributed to anatase. Upon calcination at 650 °C, no evidence of anatase peaks, except for the one located at 25.1° 2 $\theta$  are observed; however, peaks located at 27.4°, 41.2°, 44.1° and 54.3° 2 $\theta$  corresponding to rutile phase are observed. Furthermore, two additional peaks at 38.2° and 44.4° 2 $\theta$  assigned to metallic Ag (JCPDS 87-0720) also became visible.

### 3.1.2 Surface chemical analysis by XPS

Figure 2 presents the high resolution Ag(3d) spectra of Ag-TiO<sub>2</sub> films calcined at 250, 450 and 650 °C. The Ag(3d<sub>5/2</sub>) and Ag(3d<sub>3/2</sub>) peaks at ~367.8 and ~373.8 eV, respectively, are observed for Ag-TiO<sub>2</sub> films calcined at 250 °C. The same peaks are observed at ~368.1 and 374.2 eV, respectively, for the Ag-TiO<sub>2</sub> films calcined at 450 °C. When the calcination temperature further increased to 650 °C, no Ag(3d) peaks are observed. The chemical state of silver in the Ag-TiO<sub>2</sub> coating as a function of calcination temperature can be elucidated from this XPS data. It is worth mentioning that the Ag(3d) peak positions shift to higher binding energy values with increasing temperature (e.g. 250 °C vs. 450 °C). This

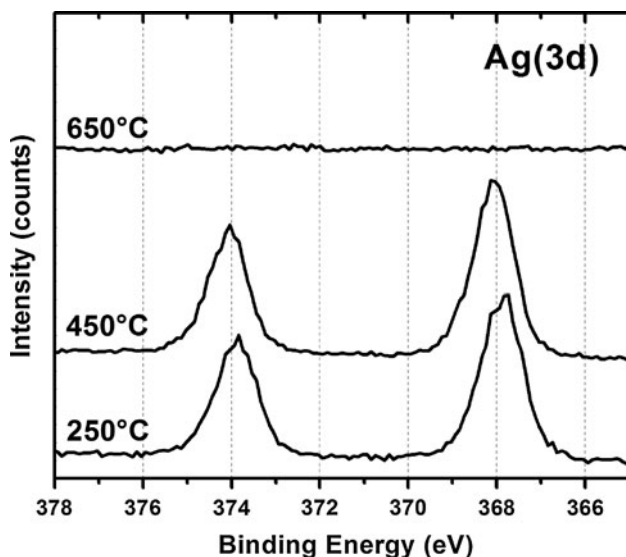


**Fig. 2** High resolution regional Ag(3d) XPS spectra of Ag-TiO<sub>2</sub> thin films calcined at 250, 450 and 650 °C

indicates that silver mostly remains in the ionic state at relatively low calcination temperatures and metallic silver (Ag<sup>0</sup>) nanoparticles start to form at higher temperatures upon thermal reduction.

## 3.2 Functional properties of thin films: bactericidal activity

### 3.2.1 Disk diffusion assay

The images in Fig. 3 show the bactericidal activity, after 24 h surface-bacteria interaction, for the control sample (bare silica pre-coated float glass), TiO<sub>2</sub> and Ag-TiO<sub>2</sub> films calcined at 250, 450 and 650 °C. The observable linear marks are bacteria colonies formed through coagulation of bacteria cells in/on the agar. The bactericidal activity of films was evaluated from changes in concentration of bacterial colonies on the surface of the film and in the surrounding region, extending from sample edge through the bacteria-seeded agar. The presence and the size of these inhibition zones, defined as areas free of bacteria or where bacterial growth is prevented, reflect the bactericidal activity.

As shown in Fig. 3, no inhibition zone is observable for the control sample (Fig. 3a) or any of the TiO<sub>2</sub> films (Fig. 3b–d). However, the surface of the TiO<sub>2</sub> films calcined at 250 °C (Fig. 3b) and 450 °C (Fig. 3c) are only partially covered by bacteria while the control sample and the TiO<sub>2</sub> thin film calcined at 650 °C are covered by bacteria. This suggests that both the 250 and 450 °C calcined films at least exhibit some bactericidal activity. Furthermore, the area of the bacteria-free region on the 450 °C-calcined TiO<sub>2</sub> film surface is relatively larger than the 250 °C sample.

In comparison, (1) Ag-TiO<sub>2</sub> thin film calcined at 250 °C showed incomplete inhibition zones of 1–2 mm in size, and (2) for Ag-TiO<sub>2</sub> films calcined at 450 °C, 3–6 mm wide, inhibition zone can be clearly seen. However, (3) Ag-TiO<sub>2</sub> films calcined at 650 °C exhibit no inhibition zone. The surfaces on the Ag-TiO<sub>2</sub> thin films calcined to 250 and 450 °C are bacteria free while the Ag-TiO<sub>2</sub> thin film calcined to 650 °C is completely covered with bacteria.

### 3.2.2 UV-induced bactericidal test

Figure 4a–c shows images indicating the bactericidal activity of the control sample, TiO<sub>2</sub> and Ag-TiO<sub>2</sub> thin films (both calcined at 450 °C) after 3, 6 and 12 h UV irradiation, respectively. As shown in Fig. 4a, both TiO<sub>2</sub> and Ag-TiO<sub>2</sub> films exhibited bactericidal activity, with the Ag-TiO<sub>2</sub> film showing enhanced (qualitative) bactericidal performance after 3 h of UV illumination. The control sample shows lack of any bactericidal activity, suggesting

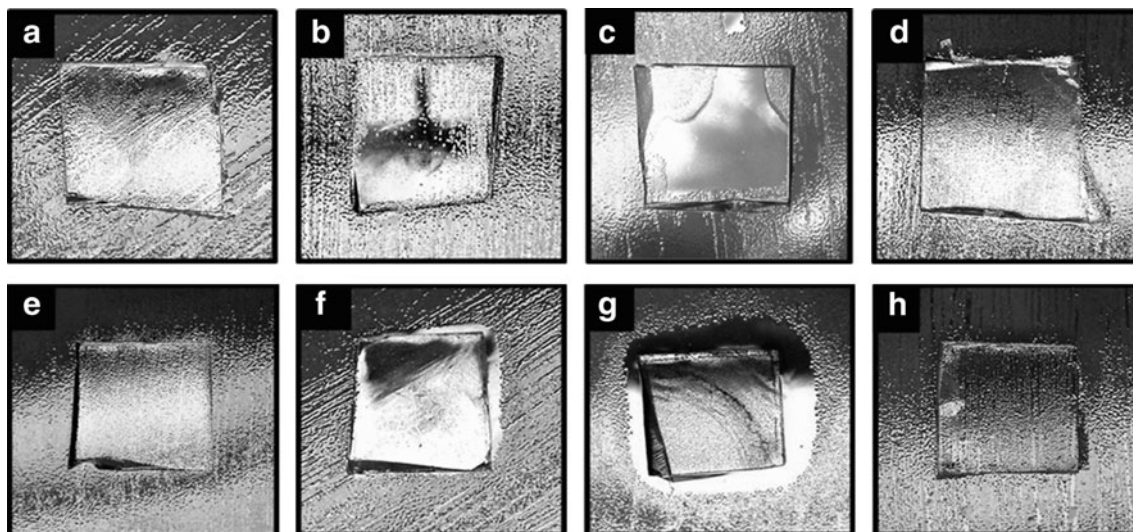


**Fig. 3** Images of antibacterial test results under natural light (ambient/visible light) against *S. epidermidis* after 24 h showing the antibacterial activity of  $\text{TiO}_2$  and  $\text{Ag-TiO}_2$  films calcined at 250 °C

(b, f), 450 °C (c, g) and 650 °C (d, h), respectively. The antibacterial activity of silica pre-coated glass samples, used as a control sample, is also shown in (a) and (e)

limited bacterial degradation solely due to UV exposure. The effect of 6 and 12 h UV exposure on the bactericidal activity of the same set of samples is shown in Fig. 4b and c. Longer UV exposure enhances the bactericidal activity for all samples including the control sample and  $\text{TiO}_2$  thin films. The evidence of increased bactericidal activity of the control sample is presumably due to natural degradation of *S. epidermidis* under excessive UV irradiation. However, the most effective bactericidal activity was again observed for  $\text{Ag-TiO}_2$  films.

In addition, Fig. 4d shows the bactericidal activity of the control sample,  $\text{TiO}_2$ , and  $\text{Ag-TiO}_2$  thin films calcined at 650 °C after 12 h UV irradiation. The number of bacteria remaining after exposure is similar for the  $\text{TiO}_2$  thin film and the control sample, however, the  $\text{Ag-TiO}_2$  thin film shows significant bactericidal activity. Comparing the second and third plates of Fig. 4c with their counterparts in Fig. 4d, it is clear that there is significant reduction in the bactericidal activity of  $\text{TiO}_2$  and  $\text{Ag-TiO}_2$  at 650 °C as compared to their counterparts calcined at 450 °C.

### 3.2.3 Qualitative Ag ion release test

Figure 5a shows the high resolution regional XPS spectra of  $\text{Ti}(2p)$  signal for the agar strip from the first set ( $\text{TiO}_2$  thin films). For the agar associated with the  $\text{TiO}_2$  films calcined at all temperatures (250, 450, and 650 °C), no Ti was found on the agar strips, indicating that Ti was not released from the films in/onto bacteria seeded agar. Figure 5b exhibits high resolution regional spectra of  $\text{Ag}(3d)$  signal for the agar strips from the second set ( $\text{Ag-TiO}_2$  thin films). Very low intensity  $\text{Ag}(3d_{5/2})$  and  $\text{Ag}(3d_{3/2})$  signals

are observed for agar associated with the  $\text{Ag-TiO}_2$  thin films calcined to 250 °C. Well defined  $\text{Ag}(3d_{5/2})$  and  $\text{Ag}(3d_{3/2})$  peaks are observed for agar strips associated with  $\text{Ag-TiO}_2$  thin film calcined to 450 °C also. Furthermore, for the agar strips associated with the  $\text{Ag-TiO}_2$  film calcined at 650 °C, no Ag signals are observed.

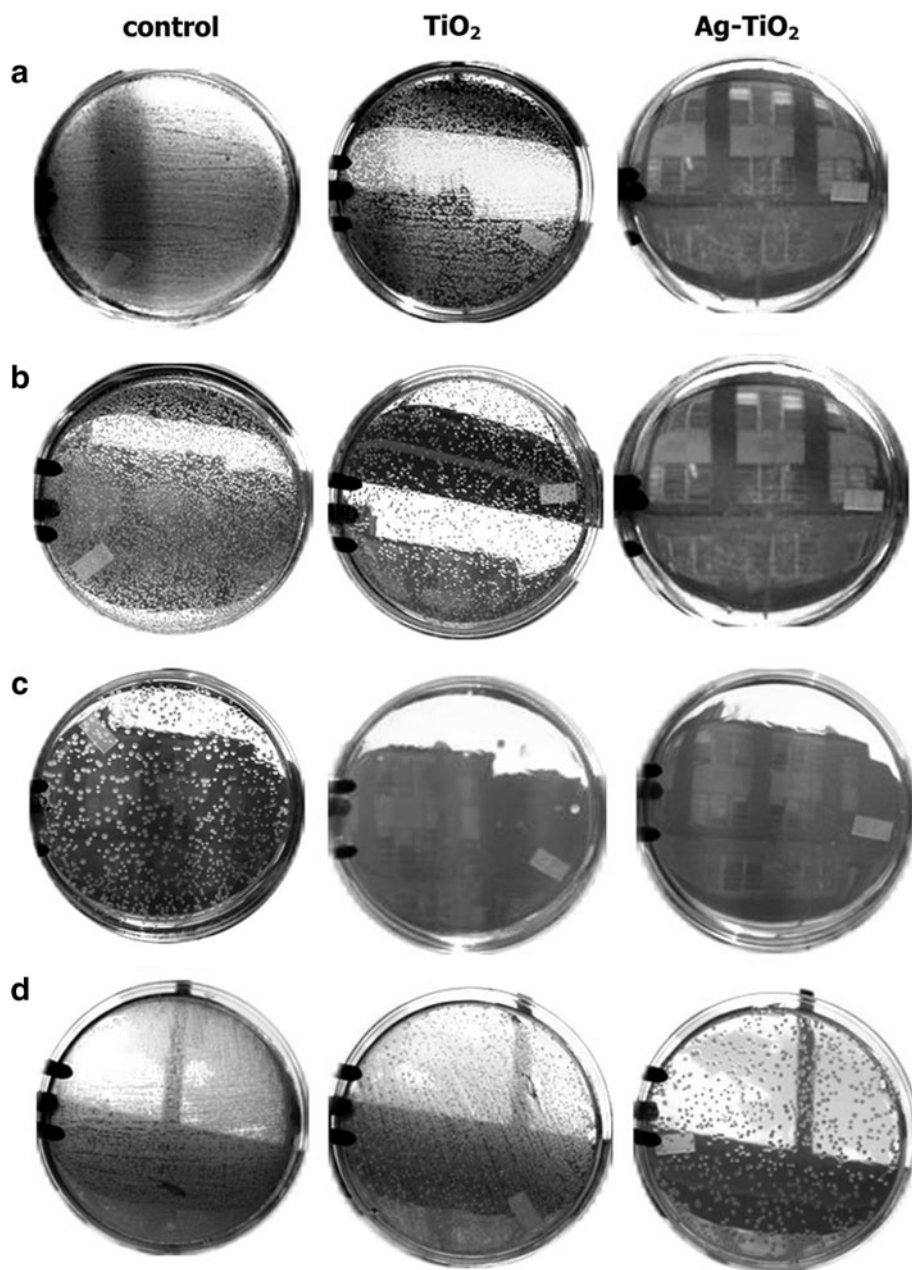
### 3.2.4 Laserscan profilometry

Figure 6 shows the representative profilometry images of the sample surfaces and also cross-sectional line profiles of the sample-agar border for the control sample,  $\text{TiO}_2$  and  $\text{Ag-TiO}_2$  films calcined at 450 °C. The small, positive relief features, represent the bacteria colonies, whereas relatively smooth surfaces represent the bacteria-free regions. In Fig. 6a, bacteria colonies are present both on the control sample surface and the region surrounding the control sample. Figure 6b shows that the  $\text{TiO}_2$  thin film surface is free of bacteria while the agar region surrounding  $\text{TiO}_2$  thin film sample was completely covered by bacteria. Figure 6c shows that the  $\text{Ag-TiO}_2$  thin film surface is free of bacteria, as is the  $\sim 2.5$  mm regions surrounding the  $\text{Ag-TiO}_2$  thin film sample.

## 3.3 Functional properties of thin films: photocatalytic activity

The IR absorption signal of stearic acid ( $2800\text{--}3000\text{ cm}^{-1}$ ) on  $\text{TiO}_2$  and  $\text{Ag-TiO}_2$  films calcined at 450 °C as a function of photoirradiation time (0–40 min) for UV, solar and visible light were collected (not shown). The area associated with the IR signal is directly proportional to the

**Fig. 4** Digital photographs of *S. epidermidis* inoculated agar plates indicating the antibacterial activity for control sample, TiO<sub>2</sub> and Ag-TiO<sub>2</sub> thin films calcined at 450 °C after UV light irradiation for **a** 3 h, **b** 6 h and **c** 12 h and **d** for the control and thin films calcined at 650 °C after 12 h UV light irradiation



amount of stearic acid remaining and thus can be converted to the percent stearic acid remaining on the film surface as a function of illumination time (Fig. 7). Under UV, solar, and visible illumination, the photocatalytic activity of the Ag-TiO<sub>2</sub> thin films was higher than that of the TiO<sub>2</sub> films. Stearic acid deposited on the TiO<sub>2</sub> film was completely degraded in 44, 55, and 86 min of UV, solar, and visible light illumination, respectively. Stearic acid deposited on the Ag-TiO<sub>2</sub> film was completely degraded in 22, 32, and 62 min of UV, solar, and visible light illumination, respectively.

Figure 8 shows the effect of calcination temperature on photocatalytic activity of Ag-TiO<sub>2</sub> films under UV

illumination. After 60 min of UV irradiation ~52% of the stearic acid remained on the Ag-TiO<sub>2</sub> thin film calcined at 250 °C. After 27 min of UV irradiation all of the stearic acid had been degraded on the Ag-TiO<sub>2</sub> thin film calcined at 450 °C. After 60 min of UV irradiation ~62% of the stearic acid remained on the Ag-TiO<sub>2</sub> thin film calcined at 650 °C.

#### 4 Discussion

The primary objective of the work was to develop a multifunctional thin film that could perform with high



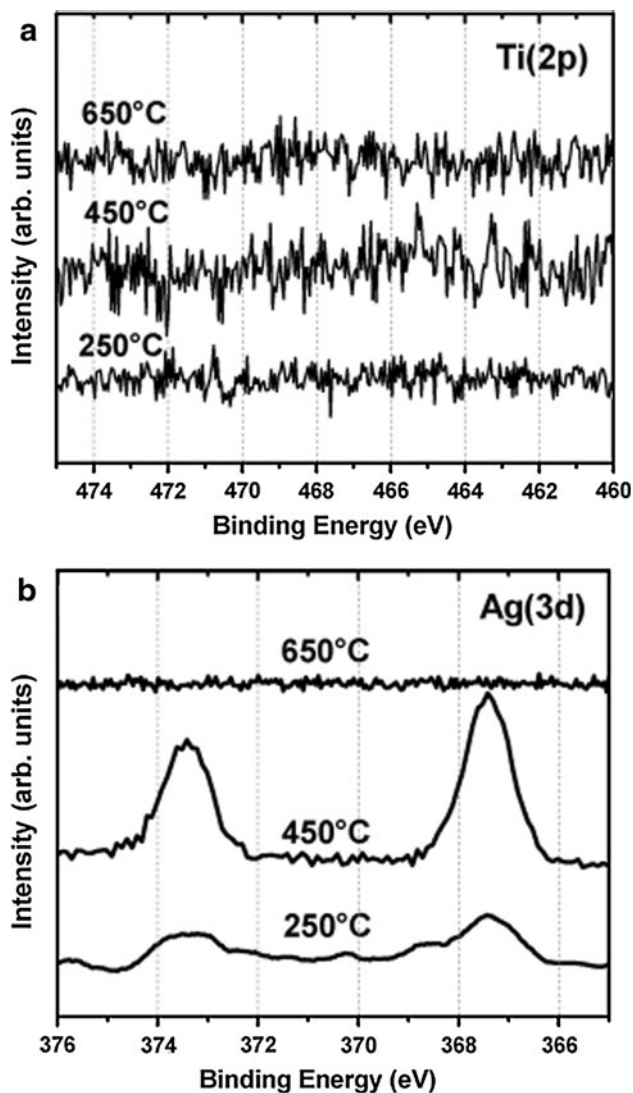


**Fig. 5** High resolution regional **a** Ti(2p) and **b** Ag(3d) XPS spectra of agar strips extracted from the area immediately surrounding the TiO<sub>2</sub> and Ag-TiO<sub>2</sub> thin films calcined at 250, 450 and 650 °C, respectively

efficiency as both a bactericidal and photocatalytic material under both natural and UV light. The performance related findings indicate both of these functional properties were related with structural properties of the films and were (1) a function of the calcination temperature and (2) improved with the incorporation of Ag into the TiO<sub>2</sub> film.

#### 4.1 Bactericidal activity

##### 4.1.1 Role of calcination temperature

GIXRD analyses showed that the TiO<sub>2</sub> thin films calcined to 250 °C were amorphous (Fig. 1) and were not antibacterial under any conditions. The marginal bactericidal activity for amorphous TiO<sub>2</sub> has been related to structural

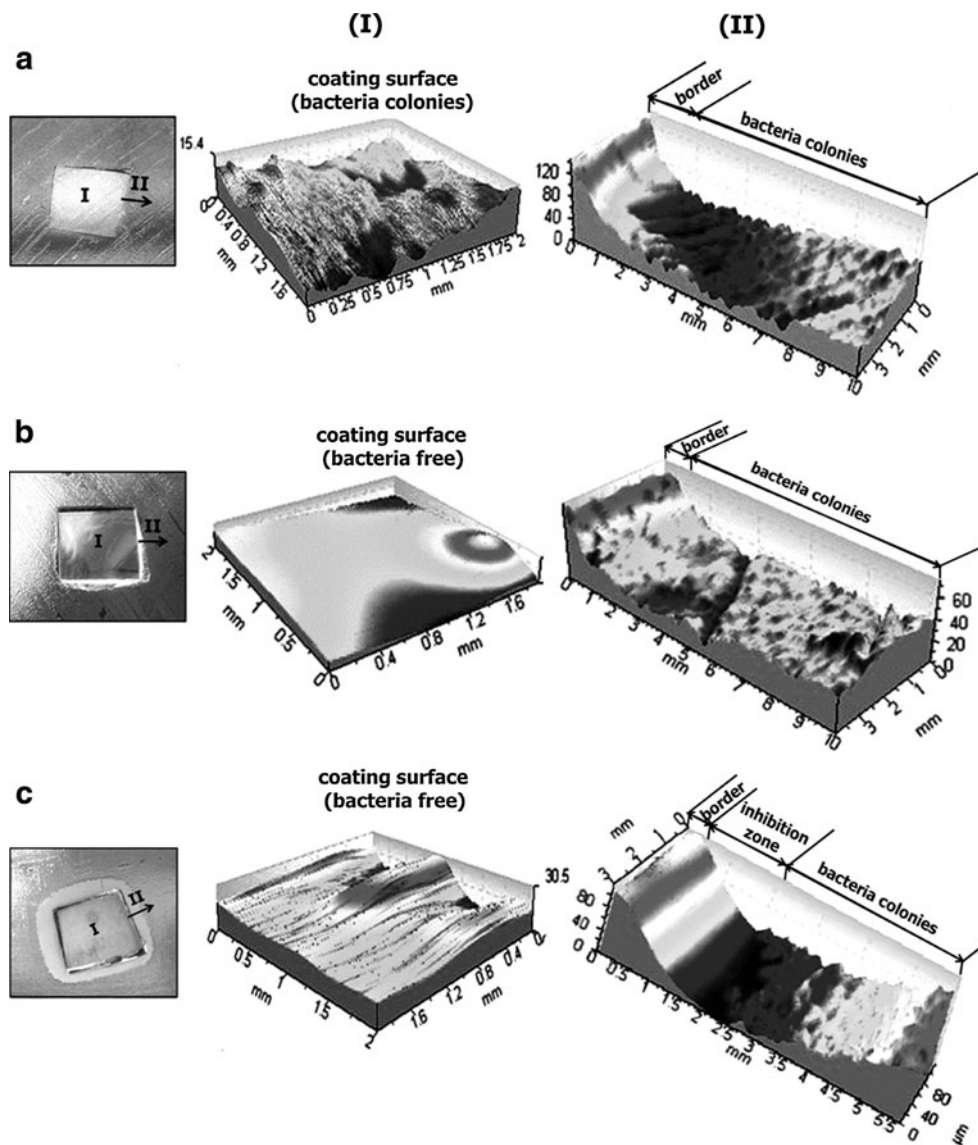
imperfections, such as microvoids, within the amorphous structure [17]. These imperfections are thought to generate additional electronic states facilitating recombination of photoexcited (e<sup>-</sup>/h<sup>+</sup>) pairs, leading to negligible production of OH<sup>-•</sup> reactive species, and hence resulting in very limited bactericidal activity [17]. An increase in calcination temperature from 250 to 450 °C leads to crystallization (anatase) of the TiO<sub>2</sub> thin film and results in the observed bactericidal effect under natural (ambient day light) and UV light. It has been shown that anatase is highly photocatalytic, therefore it is not surprising that anatase also exhibits bactericidal activity, even under natural light conditions [18–21]. Further increase in the calcination temperature to 650 °C of the TiO<sub>2</sub> thin films results in a mixed phase, anatase/rutile thin film. This TiO<sub>2</sub> thin film of mixed phase was not bactericidal under UV or natural light.

GIXRD analyses show that the Ag-TiO<sub>2</sub> thin films calcined to 250 °C are also amorphous, although a very broad peak centered around 25.3 2θ suggests the onset of anatase crystallization (Fig. 1). For the same film the XPS peak positions of Ag (3d<sub>5/2</sub>) and Ag (3d<sub>3/2</sub>) signals were recorded as 367.8 and 373.8 eV suggesting the presence of Ag<sub>2</sub>O within the film (Fig. 2). Ag-TiO<sub>2</sub> thin films calcined at 250 °C show some bactericidal activity under both natural (Figs. 3, 5) and UV light (not shown) presumably due to the Ag<sup>+</sup> release. An increase in calcination temperature from 250 to 450 °C leads to crystallization (anatase) of the TiO<sub>2</sub> thin film (Fig. 1). For this film, Ag (3d<sub>5/2</sub>) and Ag (3d<sub>3/2</sub>) peak positions shift to higher binding energy values of 368.1 and 374.2 eV, respectively, indicating thermal reduction of Ag<sup>+</sup> ions to Ag<sup>0</sup>, i.e. metallic silver (Fig. 2). However, the 450 °C calcined Ag-TiO<sub>2</sub> thin films are highly bactericidal under natural (Figs. 3, 5, 6) and UV (Fig. 4) light due to both the highly crystalline anatase structure and Ag<sup>0</sup>. Further increase in the calcination temperature to 650 °C of the Ag-TiO<sub>2</sub> thin films results in nearly pure rutile thin films (Fig. 1) without any Ag on the surface (Fig. 2). It is believed when calcined at 650 °C, Ag is not observed on the surface due to migration into the bulk of the TiO<sub>2</sub> films as a result of ionic exchange between mobile glass components (Ca<sup>2+</sup>, Na<sup>+</sup>) and Ag<sup>+</sup> [15]. No observable bactericidal activity is observed for Ag-TiO<sub>2</sub> thin films calcined at 650 °C under natural light (Figs. 3, 5) however, minimal bactericidal activity is observed under UV light (Fig. 4).

##### 4.1.2 Role of Ag

The disk diffusion assay test results (Fig. 3) showed that the addition of Ag enhances bactericidal activity under natural light conditions of TiO<sub>2</sub> films when calcined at 250 and 450 °C. The assays demonstrated absence of inhibition

**Fig. 6** Laser profilometry images of (I) agar region covering the sample surface, and (II) cross-sectional line profiles of the sample-agar border for **a** control sample, **b** TiO<sub>2</sub> and **c** Ag-TiO<sub>2</sub> thin films calcined at 450 °C



zone for the undoped TiO<sub>2</sub> films, whereas their counterparts with Ag (Ag-TiO<sub>2</sub> films) culminated in a bacteria free inhibition zone (~1–6 mm). This is consistent with other studies reporting a superior antibacterial activity of Ag-TiO<sub>2</sub> films over TiO<sub>2</sub> films [9, 22–26]. The absence of inhibition zones within the disk diffusion assay test results of TiO<sub>2</sub> film can be considered as evidence for lack of antibacterial activity under ambient and visible light conditions. However, detailed examination of the thin film surface and sample/agar interfacial region via laser profilometry suggests otherwise (Fig. 6). The agar surfaces covering the TiO<sub>2</sub> and Ag-TiO<sub>2</sub> films were found to be smooth, optically clear and free of any bacterial growth, while the surface of the control samples were rough, optically hazy, and covered with bacteria colonies. This suggests that the undoped TiO<sub>2</sub> thin film were at minimum marginally antibacterial.

Similar to antibacterial tests obtained by disk diffusion assays, the UV based antibacterial tests also show improvement in antibacterial activity upon incorporation of Ag into TiO<sub>2</sub> films. First of all, for TiO<sub>2</sub> films calcined at 450 °C, presence of Ag gave rise to considerable shortening in inactivation times (from 12 to 3 h) required for bacterial cell elimination. The significant improvement in antibacterial activity seems to be related to the presence of Ag, leading to operation of the Ag-induced antibacterial mechanism, in addition to antibacterial effect of TiO<sub>2</sub> through photocatalytic attack. It is worth noting UV light alone is harmful to bacteria, as evidenced by the UV destruction of bacteria on the control sample shown in Fig. 4d. However, our results show that the degradation of bacteria due to UV exposure is only evident with prolonged exposure, as only a marginal decrease in bacterial growth was observed after 3 h, with significant bacterial

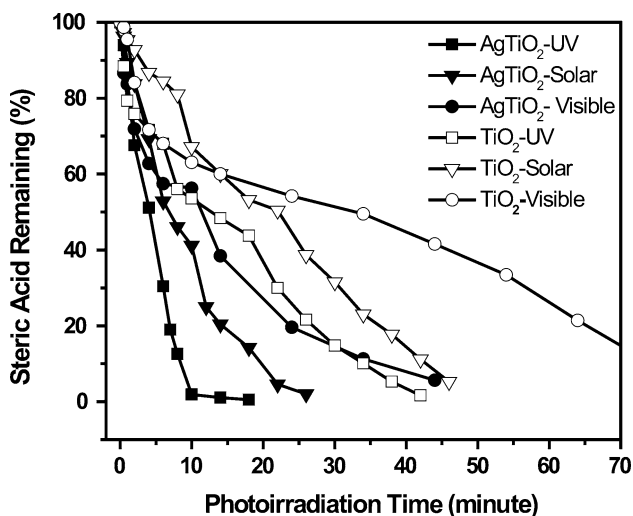


**Fig. 7** Percentage of stearic acid remaining on TiO<sub>2</sub> and Ag-TiO<sub>2</sub> films calcined at 450 °C, under illumination with UV, solar and visible light

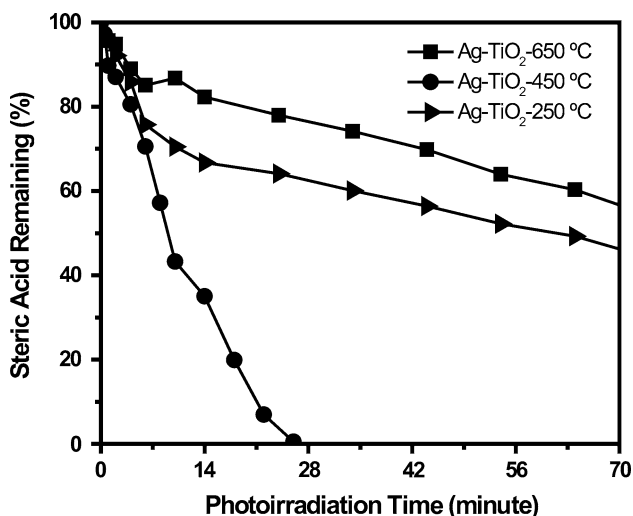


**Fig. 8** Percentage of stearic acid remaining on Ag-TiO<sub>2</sub> films calcined at 250, 450 and 650 °C under UV light illumination

degradation observed only after 12 h of photoirradiation. However, the loss of bacterial cells on the control sample (i.e. due solely to the UV light) after 12 h was minimal when compared with the destruction of bacteria on TiO<sub>2</sub> and Ag-TiO<sub>2</sub> films irradiated for 12 h under identical conditions.

**Table 1** Photocatalytic degradation rate constants (*k*) for stearic acid breakdown on TiO<sub>2</sub> and Ag-TiO<sub>2</sub> thin films calcined at 450 °C under illumination with UV, solar and visible light

Sample	UV light irradiation	Solar light irradiation	Visible light irradiation
TiO <sub>2</sub>	0.06 ± 0.01	0.03 ± 0.01	0.02 ± 0.01
Ag-TiO <sub>2</sub>	0.08 ± 0.01	0.06 ± 0.01	0.03 ± 0.01

#### 4.2 Photocatalytic activity

All TiO<sub>2</sub> and Ag-TiO<sub>2</sub> thin films were photocatalytic under UV, solar, and visible light. Under each illumination condition, addition of Ag to the TiO<sub>2</sub> thin film resulted in an increase in photocatalytic activity. For all films, under all illumination conditions, the kinetics of stearic acid breakdown can be modeled as pseudo first order. The trend in stearic acid amount as a function of time was determined via calculation of the rate constant using a pseudo first order kinetic equation: [27, 28]

$$[SA]_t = [SA]_{\text{initial}} \exp(-k \cdot t)$$

where [SA]<sub>t</sub> is the remaining stearic acid amount after distinct time *t* of illumination, [SA]<sub>initial</sub> is the initial amount of stearic acid, and *k* is the rate constant.

The photocatalytic reaction rates of TiO<sub>2</sub> and Ag-TiO<sub>2</sub> under UV, solar and visible light is shown in Table 1. For TiO<sub>2</sub> film, the photocatalytic reaction rate of stearic acid under UV light illumination was 0.06 ± 0.01 min<sup>-1</sup>, and increased to 0.08 ± 0.01 min<sup>-1</sup> with addition of Ag. The same trend was observed under solar and visible light illumination after incorporation of Ag into the TiO<sub>2</sub> films (Table 1); The photocatalytic reaction rate of stearic acid under solar and visible light illumination was found to increase from 0.03 ± 0.01 and 0.02 ± 0.01 min<sup>-1</sup>, to 0.06 ± 0.01 and 0.03 ± 0.01 min<sup>-1</sup>, respectively.

In order to further understand the role of thin film structure of photocatalytic activity the effect of calcination temperature on photocatalytic activity of Ag-TiO<sub>2</sub> thin films was determined under UV illumination (Fig. 8; Table 2). The photodegradation rate of stearic acid was; 0.011 ± 0.005, 0.080 ± 0.006, and 0.017 ± 0.006 min<sup>-1</sup> for Ag-TiO<sub>2</sub> films calcined at 250, 450 and 650 °C, respectively (Table 2).

**Table 2** Photocatalytic degradation rate constants (*k*) for stearic acid breakdown on Ag-TiO<sub>2</sub> thin films calcined at 250, 450 and 650 °C under UV illumination

Sample	UV light irradiation
Ag-TiO <sub>2</sub> calcined at 250 °C	0.011 ± 0.005
Ag-TiO <sub>2</sub> calcined at 450 °C	0.080 ± 0.006
Ag-TiO <sub>2</sub> calcined at 650 °C	0.017 ± 0.006

## 5 Conclusions

Sol–gel based TiO<sub>2</sub> and Ag-incorporated TiO<sub>2</sub> thin films were formed by spin coating and their bactericidal and photocatalytic activities were measured under various illumination conditions. It was found that all TiO<sub>2</sub> and Ag-TiO<sub>2</sub> thin films calcined at 450 °C were both bactericidal and photocatalytically active under all illumination conditions investigated. Additionally, under any given illumination condition the Ag-doped films were found to have increased bactericidal and photocatalytic activity compared to TiO<sub>2</sub> thin films. Bactericidal and photocatalytic activity was shown to be a function of thin film structure and chemistry, with optimized performance obtained with Ag-TiO<sub>2</sub> thin films after calcination at 450 °C.

**Acknowledgments** Supported by The Scientific and Technological Research Council of Turkey (TUBITAK) under 106M061 Grant, Alfred University, and the 3M Non-Tenured Faculty Grant (NPM). BAA also thanks TUBITAK for the support through 2214 National Scholarship Program for PhD students. The authors wish to thank Brain Adams for his assistance in XPS.

## References

- Hoffmann MR, Martin ST, Choi W, Bahnemann DW (1995) *Chem Rev* 95:69–96
- Tang WZ, An H (1995) *Chemosphere* 31:4171–4183
- Herrmann JM, Tahiri H, Ait-Ichou Y, Lassaletta G, Gonzalez-Elipe AR, Fernandez A (1997) *Appl Catal B-Environ* 13:219–228
- Liu SX, Qu ZP, Han XW, Sun CL (2004) *Catal Today* 93–95:877–884
- Tran H, Scott J, Chiang K, Amal R (2006) *J Photoch Photobio A* 183:41–52
- Ao Y, Xu J, Fu D, Yuan C (2008) *J Phys Chem Solids* 69: 2660–2664
- Akhavan O (2009) *J Colloid Interf Sci* 336:117–124
- Kato S, Hirano Y, Iwata M, Sano T, Takeuchi K, Matsuzawa S (2005) *Appl Catal B-Environ* 57:109–115
- Page K, Palgrave RG, Parkin IP, Wilson M, Savin SLP, Chadwick AV (2007) *J Mater Chem* 17:95–104
- Tanahashi I (2007) *B Chem Soc Jpn* 80:2019–2023
- Bansal A, Madhavi S, Yang Tan TT, Lim TM (2008) *Catal Today* 131:250–254
- Li H, Zhao G, Song B, Han G (2008) *J Clust Sci* 19:667–673
- Kafizas A, Kellici S, Darr JA, Parkin IP (2009) *J Photoch Photobio A* 204:183–190
- Guglielmi M, Brusatin G, Tombolan N (1993) Ion migration in thin sol-gel glass coatings. Proceedings of the Second Conference of the Europ Soc of Glass Sci and Technol, pp 495–498
- Akkopru Akgun B, Durucan C, Mellott NP (2011) *J Sol-Gel Sci Tech* 58:277–289
- Mellott NP, Durucan C, Pantano CG, Guglielmi M (2006) *Thin Solid Films* 502:112–120
- Ohtani B, Ogawa Y, Nishimoto S (1997) *J Phys Chem B* 101:3746–3752
- Sclafani A, Palmisano L, Davi E (1991) *New J Chem* 14:265–268
- Kavan L, Grätzel M, Gilbert SE, Klemenz C, Scheel HJ (1996) *J Am Chem Soc* 118:6716–6723
- Benabbou AK, Derriche Z, Felix C, Lejeune P, Guillard C (2007) *Appl Catal B-Environ* 76:257–263
- Brook LA, Evans P, Foster HA, Pemble ME, Steele A, Sheel DW, Yates HM (2007) *J Photoch Photobio A* 187:53–63
- Sokmen M, Candan F, Sumer Z (2001) *J Photoch Photobio A* 143:241–244
- Machida M, Norimoto K, Kimura T (2005) *J Am Ceram Soc* 88:95–100
- Coleman HM, Marquis CP, Scott JA, Chin S-S, Amal R (2005) *Chem Eng J* 113:55–63
- Kubacka A, Ferrer M, Martínez-Arias A, Fernández-García M (2008) *Appl Catal B-Environ* 84:87–93
- Yang C, Liang GL, Xu KM, Gao P, Xu B (2009) *J Mater Sci* 44:1894–1901
- Sawunyama P, Jiang L, Fujishima A, Hashimoto K (1997) *J Phys Chem B* 101:11000–11003
- Yu J, Zhao X, Zhao Q (2001) *Mater Chem Phys* 69:25–29